

The chiral phase transition and equation of state in the chiral imbalance

Qing-Wu Wang,^{1,*} Chao Shi,^{2,†} and Hong-Shi Zong^{3,4,5,‡}

¹College of Physics, Sichuan University, Chengdu 610064, China

²Department of nuclear science and technology, Nanjing University of Aeronautics and Astronautics, Nanjing 210016, China;

³Department of Physics, Nanjing University, Nanjing 210093, China

⁴Department of Physics, Anhui Normal University, Wuhu, Anhui 241000, China

⁵Nanjing Institute of Proton Source Technology, Nanjing 210046

The chiral phase transition and equation of state are studied within a new self-consistent mean-field approximation of the two-flavor Nambu–Jona-Lasinio model. In this newly developed model, modifications to the chemical potential μ and chiral chemical potential μ_5 is naturally included by adding vector and axial-vector channels from Fierz-transformed Lagrangian to the standard Lagrangian. In proper-time scheme, the chiral phase transition is a crossover in the $T - \mu$ plane. But when μ_5 is increased, our study shows that there may exist first order phase transition. Furthermore, the chiral imbalance will soften the equation of state of quark matter. The mass-radius relations and tidal deformability of quark stars are calculated. As μ_5 increases, the maximum mass and radius decrease. The vector channel and axial-vector channel have opposite influence on the equation of state. However, when EOS is constrained by astronomical observations, the shape of the mass-radius curve can be used to determine whether there is chiral imbalance in the dense object, and thus indirectly proving the CP violation in the dense matter. Our study shows a different influence of the chiral imbalance on the chiral phase transition in contrary to tree-momentum-cutoff scheme.

I. INTRODUCTION

The phase diagram of strongly interacting matter is an important topic in hadron physics. Under extreme conditions, the hadron state will undergo phase transition from hadron to quark and the restoration of spontaneous chiral symmetry [1–4]. At finite temperature and finite density, the chiral restoration may be a first-order phase transition, but the results of different models and even different regularization are inconsistent. At zero baryon density, the lattice Monte Carlo simulations give reliable result that the chiral transition is a crossover, but when the temperature is zero and the density is high, the lattice calculation faces the sign problem [5, 6].

At high density, topological gauge fields with nonzero winding number (instantons and sphalerons) may appear [7–12]. The interaction of quarks with these topological gauge fields will change the helicities of the quarks, which results in the chiral imbalance between left- and right-hand quarks via the axial anomaly [13–15]. The interaction of quarks with these topological gauge fields would also lead to a local P and CP violation. The strong magnetic fields are suggested to be produced at the very first moments of a noncentral heavy ion collision [16, 17]. If the chiral imbalance is obvious here, it will result in the observable effects in experiment since the right- and left-hand quarks move in different directions along the magnetic field. This phenomenon is called as chiral magnetic effect (CME) [20] and can be served as indirect evidence for P and CP violation [18, 19].

The chiral imbalance means an asymmetry in the number of right- and left-handed quarks which. In order to study the effect of this asymmetry, a chiral chemical potential μ_5 that

conjugated to the chiral charge density n_5 , can be introduced [20, 21]. As showed in Refs. [21–23], this chiral chemical potential affect the position of critical end point (CEP). Furthermore, on the theoretical side, the exist and location of CEP depend on models and regularisation. To confirm and find the CEP is a hot issue [24–26]. Even if CEP exists, its location is still uncertain. People expect to give relevant information from experiments [27–30] and astronomy [31–34].

Before the study of chiral phase transition, an appropriate regularisation scheme must be chosen. The CEP exists in the three-momentum cutoff scheme but disappears in the proper-time regularisation scheme. So it is wonder whether the CEP exists in a chiral imbalance system. We will exam if the existence of chiral imbalance could lead to the chiral phase transition from crossover to a first-order transition. If the first-order phase transition is found in QGP but without properly regulation of the chirally imbalance, it is still uncertain whether the first-order transition is caused by high density or chiral imbalance.

Since the chiral imbalance changes the possible location of CEP, it will naturally affect the equation of state (EOS). However, because the quantum anomaly in defining chiral density, n_5 is not a strictly conserved quantity. So studies on chiral imbalance effect is considered as on a time scale much larger than the typical time scale of the chirality changing processes [35]. And the possible impact of chiral imbalance on the EOS is neglected on the literature. But chiral density may induce by electro-magnetic fields. As showed in the Eq. (1) in Ref. [35] with parallel magnetic fields in the background, the chiral density n_5 is proportional to the magnetic field strength. We known that pulsars are found with strong magnetic field. Thus chiral imbalance has a greater probability of occurrence in pulsars and CME will be more obvious. In this paper, we will firstly study the effect of chiral imbalance on the equation of state (EOS) under proper-time regularization. Furthermore, the influence on the mass-radius relations and tidal deformability of quark stars will be investigated and hope to find some

*Electronic address: qw.wang@scu.edu.cn

†Electronic address: shichao0820@gmail.com

‡Electronic address: zonghs@nju.edu.cn

clue for CP violation in compact object.

In this paper, the chiral phase transition is studied under the recent developed NJL model with proper-time regularization [36–38]. The standard two-flavor Nambu–Jona-Lasinio (NJL) Lagrangian contains only scalar and pseudoscalar-isovector channels. But its Fierz transformation, as a mathematically equivalence, contains more interactive channels [39], especially the vector channel. Except the chiral chemical potential, model calculations show that the vector channel will also affect chiral phase structure and the location of CEP [40, 41]. The critical chemical potential will increase as the vector coupling increases. When the coupling is larger enough, the CEP will disappear. The contribution from the vector channel is quite important at nonzero densities. The strength of the vector coupling is usually taken as free parameter in quark model. In the relativistic mean-field model of nuclear matter, the vector couplings are fitted to low-energy data. But whether it would be suppressed at high temperature and high density is unknown. Then density-dependent couplings are proposed in the exploring of hot and dense nuclear matter. Therefore, the detection of CEP in heavy-ion collisions will also provide information about vector channel interactions.

The linear combination of standard NJL Lagrangian and its Fierz transformation will include the vector channels interaction in a consistent way. The concerned channels in the Fierz transformation are the vector channel $-(\bar{\psi}\gamma^\mu\psi)^2$ and the axial-vector channel $-(\bar{\psi}i\gamma_5\gamma^\mu\psi)^2$. In the mean-field-approximation,

$$-(\bar{\psi}\gamma^\mu\psi)^2 \approx -2n\psi^\dagger\psi + n^2, \quad (1)$$

$$-(\bar{\psi}i\gamma_5\gamma^\mu\psi)^2 \approx 2n_5\psi^\dagger\gamma_5\psi - n_5^2. \quad (2)$$

Here, the n and n_5 are the number density and the chiral number density of quarks respectively.

This paper is organized as follows: In Sec. II, we introduce the newly developed self-consistent mean-field theory of the NJL model. In Sec. III, We give our numerical results and analysis on the phase transition. Sec. IV is a short summary of our work.

II. NAMBU–JONA-LASINIO MODEL

In the recently developed self-consistent two-flavor NJL model [36–38], the Lagrangian can be expressed as a linear combination of a standard NJL Lagrangian (\mathcal{L}_{NJL}) and its Fierz transformation (\mathcal{L}_{Fierz}) [2, 39, 42], that is

$$\mathcal{L}_C = (1 - \alpha)\mathcal{L}_{NJL} + \alpha\mathcal{L}_{Fierz}, \quad (3)$$

where α weights the contribution from Fierz transformation. At finite density, $\mu\psi^\dagger\psi$ can be added to the right of Eq. (3). Similarly, we can consider quark chiral imbalance by adding a term $\mu_5\psi^\dagger\gamma_5\psi$ to the right side with μ_5 being the chiral chemical potential coupling to the chiral operator. Here, we use the standard NJL Lagrangian with four-quark interaction for

\mathcal{L}_{NJL} . The \mathcal{L}_{NJL} and its Fierz transformation \mathcal{L}_{Fierz} can be written, respectively, as

$$\mathcal{L}_{NJL} = \bar{\psi}(i\cancel{\partial} - m)\psi + G[(\bar{\psi}\psi)^2 + (\bar{\psi}i\gamma_5\bar{\tau}\psi)^2], \quad (4)$$

and

$$\begin{aligned} \mathcal{L}_{Fierz} = & \bar{\psi}(i\cancel{\partial} - m)\psi + \frac{G}{8N_c}[2(\bar{\psi}\psi)^2 + 2(\bar{\psi}i\gamma_5\bar{\tau}\psi)^2 \\ & - 2(\bar{\psi}\bar{\tau}\psi)^2 - 2(\bar{\psi}i\gamma_5\psi)^2 - 4(\bar{\psi}\gamma^\mu\psi)^2 \\ & - 4(\bar{\psi}i\gamma^\mu\gamma_5\psi)^2 + (\bar{\psi}\sigma^{\mu\nu}\psi)^2 - (\bar{\psi}\sigma^{\mu\nu}\bar{\tau}\psi)^2]. \end{aligned} \quad (5)$$

Under the mean-field approximation, the effective quark mass is

$$M = m - 2G'\sigma. \quad (6)$$

Here, $\sigma = \langle\bar{\psi}\psi\rangle$ is the two-quark condensation and G' is the four-quark effective coupling for the mixed Lagrangian Eq. (3) which has the relation with G

$$G' = (1 - \alpha + \frac{\alpha}{4N_c})G. \quad (7)$$

It is the new coupling G' that needs to be recalibrated to fit the low-energy experimental data. The modified chemical potential and chiral chemical potential are defined, respectively, as

$$\mu_r = \mu - \frac{\alpha G}{N_c}n, \quad (8)$$

$$\mu_{5r} = \mu_5 + \frac{\alpha G}{N_c}n_5. \quad (9)$$

Here, $n = \langle\psi^\dagger\psi\rangle$ is the quark number density and $n_5 = \langle\psi^\dagger\gamma_5\psi\rangle$ is the chiral number density. Note here that, because the introduction of the four-quark pseudo-vector interaction are different by a negative sign here and in Eq. (31) of Ref. [21], the modified μ_5 differs by a negative sign in Eq. (9) and Eq. (34) of Ref. [21].

The chiral condensate and (chiral-) quark number densities are given by minimizing the thermodynamic potential density. At finite density and temperature, the chiral condensate is

$$\sigma = -\frac{N_c N_f M T}{2\pi^2} \sum_{s=\pm 1} \sum_{n=-\infty}^{\infty} \int \frac{\mathbf{p}^2}{E_s^2 + \tilde{\omega}_n^2} dp, \quad (10)$$

where $\tilde{\omega}_n$ is the fermion Matsubara frequency which is defined as $\tilde{\omega}_n = \omega_n + i\mu$, $\omega_n = (2n+1)\pi T$ with $n \in \mathbb{Z}$. And the energy for different helicity s is defined as $E_s = \sqrt{M^2 + (\mu_{5r} - s|\mathbf{p}|)^2}$ with $s = \pm 1$. In the proper-time regularization scheme, $1/A(p^2)$ is replaced by $\int_{\tau_{UV}}^{\infty} d\tau e^{-\tau A(p^2)}$, with $\tau_{UV} = 1/\Lambda_{UV}^2$ and Λ_{UV} is the UV cutoff to regularize the ultraviolet divergence. The chiral condensate at finite temperature and density can be written as in Ref. [43] as

$$\sigma = -\frac{N_c N_f M}{2\pi^2} \sum_{s=\pm 1} \int_0^\infty \int_{\tau_{UV}}^\infty \frac{p^2 e^{-\tau E_s^2}}{\sqrt{\pi\tau}} \times \quad (11)$$

$$[1 - f_s^-(p, \mu_r, \mu_{5r}, T) - f_s^+(p, \mu_r, \mu_{5r}, T)] d\tau dp,$$

$$= -\frac{N_c N_f M}{2\pi^2} \sum_{s=\pm 1} \int_0^\infty \frac{p^2}{E_s} \text{Erfc}(\sqrt{\tau_{UV}} E_s) \times \quad (12)$$

$$[1 - f_s^-(p, \mu_r, \mu_{5r}, T) - f_s^+(p, \mu_r, \mu_{5r}, T)] dp.$$

Here $\text{Erfc}(x)$ is the complementary error function and the f_s^\pm defines the Fermi-Dirac distribution function under the modified (chiral-) chemical potentials and nonzero temperature T , with

$$f_s^\pm = \frac{1}{1 + e^{(\omega_s \pm \mu_r)/T}}. \quad (13)$$

Similarly, the quark number density n and the chiral number density n_5 are

$$n = \frac{N_c N_f}{2\pi^2} \sum_{s=\pm 1} \int_0^\infty p^2 [f_s^-(p, \mu_r, \mu_{5r}, T) - f_s^+(p, \mu_r, \mu_{5r}, T)] dp, \quad (14)$$

$$n_5 = \frac{N_c N_f}{2\pi^2} \sum_{s=\pm 1} \int_0^\infty p^2 \frac{\mu_{5r} - s p}{E_s} \text{Erfc}(\sqrt{\tau_{UV}} E_s) [1 - f_s^-(p, \mu_r, \mu_{5r}, T) - f_s^+(p, \mu_r, \mu_{5r}, T)] dp. \quad (15)$$

With $f_\pi = 93$ MeV, $m_\pi = 135$ MeV, and $m = 3.5$ MeV, three parameters (m , G' , and τ_{UV}) are fixed to fit the Gell-Mann–Oakes–Renner relation: $-2m \langle \bar{\psi}\psi \rangle = (f_\pi m_\pi)^2$. The quark condensate is $\langle \bar{\psi}\psi \rangle^{1/3} = -282.4$ MeV. Then we have $G' = 4.1433 \times 10^{-6} \text{MeV}^{-2}$ and $\Lambda_{UV} = 955$ MeV. The coupling G is adjusted with α .

In order to study the response of chiral condensate to chemical potentials and temperature, the susceptibilities are defined by

$$\chi_\mu = -\frac{\partial \sigma}{\partial \mu}, \quad \chi_{\mu_5} = \frac{\partial \sigma}{\partial \mu_5}, \quad \text{and} \quad \chi_T = -\frac{\partial \sigma}{\partial T}. \quad (16)$$

III. RESULTS AND ANALYSIS

For different α , the pseudo-transition point is around $\mu = 300$ MeV at $T = 0$ and increases as α increases which is similar to the results from three-momentum cutoff scheme. For nonzero temperature, the χ_T is showed in Figure 1. It is crossover even when $\mu = 300$ MeV. It is different from the three-momentum cutoff scheme that the proper-time regularization scheme gives a crossover for the chiral phase transition even at vary large μ and thus CEP does not exist in the chirally balanced system ($\mu_5 = 0$) in this regularization scheme. We will show the results with $\mu_5 \neq 0$ bellow.

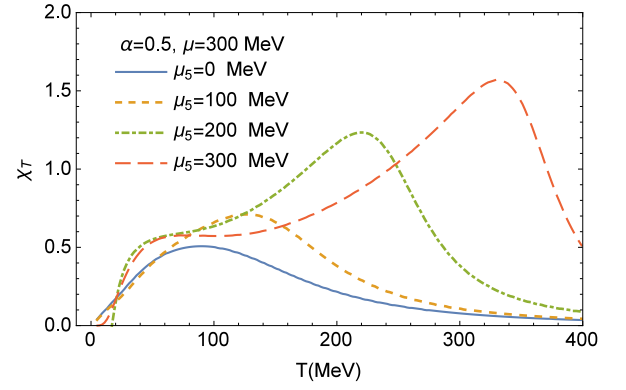


FIG. 1: The temperature susceptibility for different chiral chemical potential μ_5 .

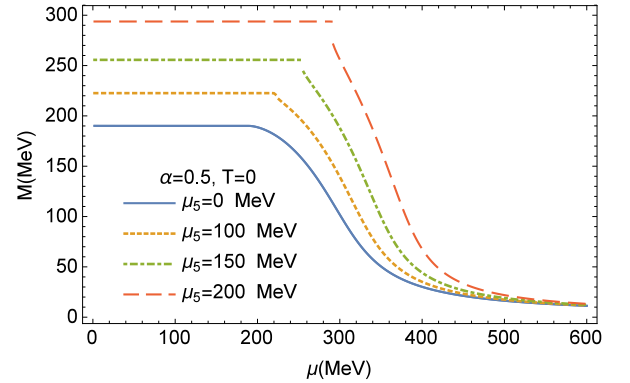


FIG. 2: The quark mass as a function of chemical potential μ for different chiral chemical potential μ_5 .

A. The exists of CEP

As chiral imbalance appeared, a jump down in the $M - \mu$ plot appears, as showed in Figure 2. The jump occurs at about $\mu = M_{vac}$ only for relatively large μ_5 , where M_{vac} is the quark mass at $T = \mu = 0$. Beside, it shows that quark mass increases for different chiral chemical potential. The phenomenon that chiral condensate increases with some external field is called ‘catalysis’. Similar to the magnetic catalysis [44–47], it may be called as chiral catalysis here since it is caused by chiral imbalance. The inverse magnetic catalysis is found [48, 49]. Here in the proper-time scheme, only chiral catalysis exists with constant couplings. In the three-momentum cutoff scheme, inverse chiral catalysis exists as the chiral symmetry is partly restored [23].

In Figure 3, the chemical susceptibilities χ_μ for different μ_5 at $T=0, 10, 20$, and 50 MeV are presented. When $\mu_5 = 0$, the chiral transition is always a crossover at any T and μ . As μ_5 is nonzero, peaks and bumps appear in the plots. When $T = 0$ and $\mu_5 > 0$, the increasing of μ will cause significant peaks in the susceptibility lines. This is a phenomenon different to results when $\mu_5 = 0$ which strongly suggests that there is a first-order phase transition. It is obvious that the critical chemical potentials increase with μ_5 . As temperature in-

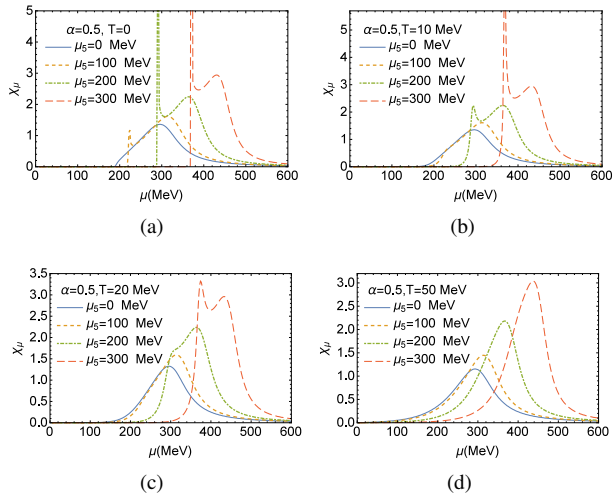


FIG. 3: The susceptibilities as a function of μ for different chiral chemical potential μ_5 and temperature T .

creases, the peaks begin to disappear even for nonzero μ_5 and remains only pumps. This change may indicate the existence of CEP in chiral imbalance system.

B. The exists of CEP₅

In order to show the influence of chiral imbalance more clearly, we show the quark mass as a function of chiral chemical potential μ_5 in Figure 4. And the corresponding susceptibilities for fixed baryon chemical potentials are also presented.

As chemical potential μ less than 200 MeV, the quark mass almost unchanged with μ but smoothly increases with chiral chemical potential μ_5 . So, the phase diagram in the $T - \mu_5$ plane is crossover in this region of μ . As $\mu \geq 220$ MeV, obvious peaks are showed up in the plot of χ_{μ_5} which implies the exists of the first order phase transition and CEP₅. The plot also shows that even if the CEP₅ exists, there is a threshold for chemical potential μ . However, since the quark condensate or mass does not change obviously here at the transition point, it is hard to find exactly where the first order phase transition begins. At $T=0$, the beginning of first order transition in the $\mu_5 - \mu$ plane is located in regions of $\mu \in (200, 220)$ MeV and close to $\mu_5 = 100$ MeV.

The critical temperature in the CEP plane will increase with temperature. Since it is also hard to locate the CEP, to find a relation of CEP and CEP₅ seems not possible in the proper-time regularization scheme. Here, we show the pseudo-critical temperature T_c and critical chemical potential μ_c ($T=0$) as a function of chiral chemical potential μ_5 in Figure 5 and Figure 6, respectively. As $\mu = \mu_5 = 0$, the pseudo-critical temperature is about 181 MeV. The T_c decreases with α which is similar to the result with three-momentum cutoff regularization. But the T_c and μ_c increase with μ_5 . This result is different from the result with three-momentum cutoff regularization. In Figure 6, both pseudo-critical and critical chemical potentials as a function of μ_5 at $T=0$ are presented. The

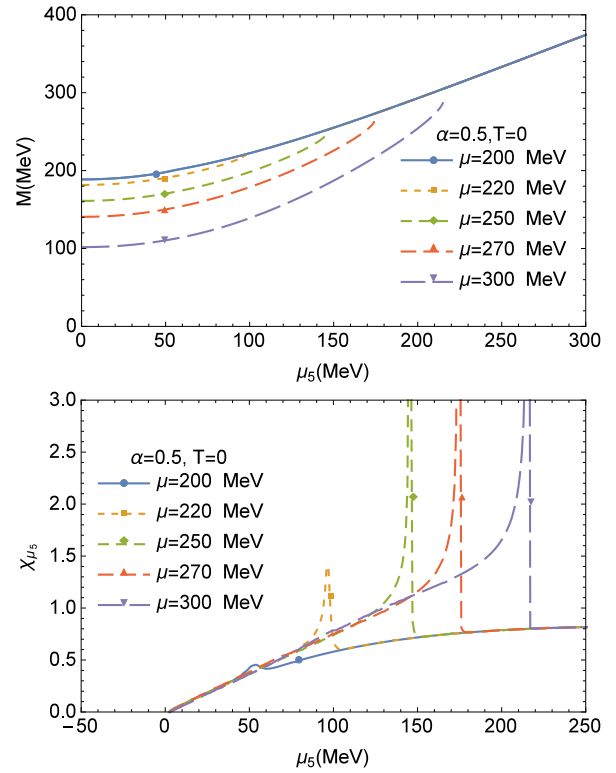


FIG. 4: Chiral catalysis effect and chiral susceptibility at zero temperature. In the up-plane, as μ_5 is larger than some critical values, lines of $\mu > 200$ MeV coincide with line of $\mu = 200$ MeV .

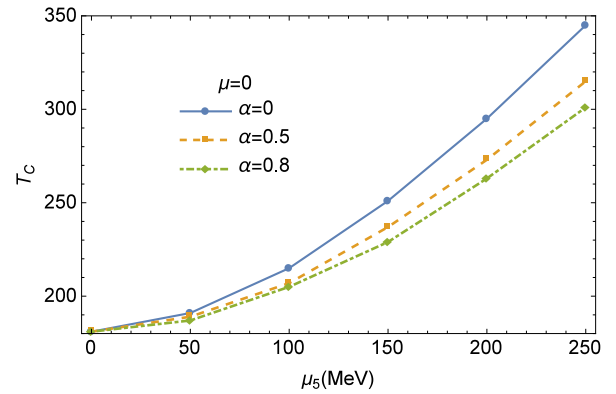


FIG. 5: The pseudo- critical temperature T_c as a function of chiral chemical potential μ_5

solid lines represent the pseudo- critical chemical potentials which are larger than the critical chemical potentials (dotted lines). No critical chemical potentials exist at small μ_5 . The pseudo- critical chemical potentials increases with α , while the critical chemical potentials increase with α . This trend can also be seen from Figure 3(a). With the increase of μ_5 , the peak and bump become close to each other. For very large μ_5 , pump disappears and only critical chemical potentials exists.

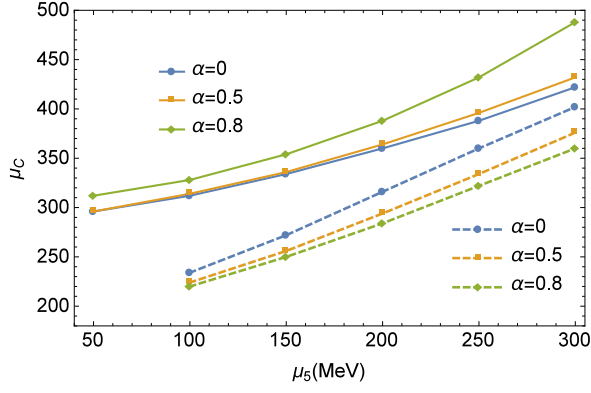


FIG. 6: The (pseudo-) critical chemical potential μ_c as a function of chiral chemical potential μ_5 . The solid lines show the pseudo critical chemical potential while the dashed lines show the critical chemical potential.

C. The EOS of quark matter in chirally imbalanced system

In the end we study the influence of chiral imbalance on the EOS of quark matter and mass-radius relation of quark stars. If first-order phase transition were found in the astronomical observation, it will confirm the exist of CEP [50, 51] and result in the emergence of a third family of compact stars, in addition to white dwarfs and neutron stars [52–54]. For quark matter, the model-independent equations of state of strong interaction matter are [55, 56]

$$P(\mu) = P_0 + \int_0^\mu d\mu n(\mu), \quad (17)$$

$$\varepsilon(\mu) = -P(\mu) + \mu n(\mu). \quad (18)$$

Here, P_0 represents the vacuum pressure at $\mu = 0$ and is taken as $P_0 = -(120 \text{ MeV})^4$. The mass of recent observed pulsars [57–60] is about $2M_\odot$. We set $\alpha = 0.8$ to ensure the EOS is stiff enough. In studying the mass-radius relation, we use the static TOV equations (in units $G = c = 1$)

$$\frac{dP(r)}{dr} = -\frac{(\varepsilon + P)(M + 4\pi r^3 P)}{r(r - 2M)}, \quad (19)$$

$$\frac{dM(r)}{dr} = 4\pi r^2 \varepsilon. \quad (20)$$

Here, P and ε are the pressure and energy density as in Eqs. (17) and (18). $M(r)$ is the quark star mass as a function of radius r . The equations are solved iteratively from a central pressure to zero pressure that defines the edge of the star [61]. Figure 7 shows that the EOS becomes soft as μ_5 increases. The maximum masses and radii of quark star reduce as μ_5 increases. When μ_5 is greater than 150 MeV, the maximum mass becomes less than $2 M_\odot$. When μ_5 is greater than 200 MeV, the maximum radius becomes less than 10 km. If the observed pulsars of masses larger than $2 M_\odot$ are identified as quark stars and radius larger than 10 km, then the chiral chemical potential cannot be very large.

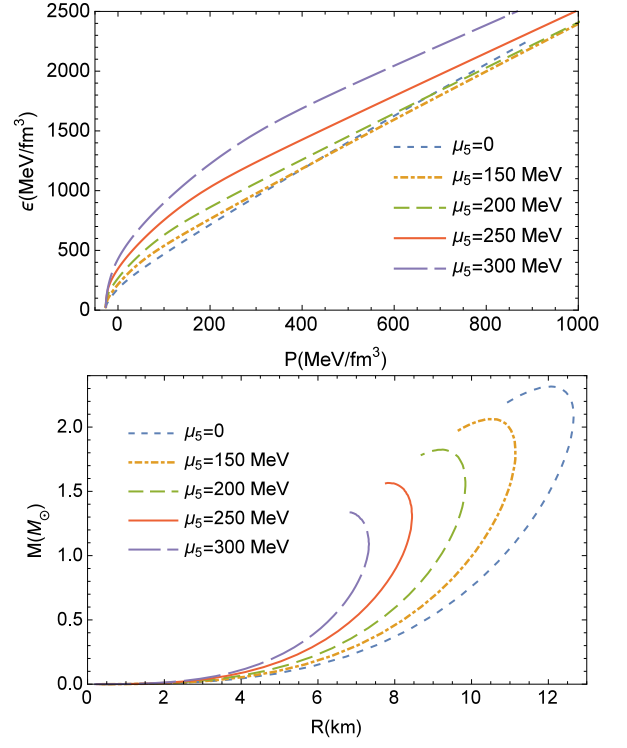


FIG. 7: The influences of chiral imbalance on the EOS of quark matter and the mass-radius relation of quark stars. The tidal deformabilities are 827.237, 421.616, 194.621, and 56.618, respectively, which decreases as μ_5 increases.

During the merger of two compact stars, the tidal formability Λ measures the star's quadrupole deformation in response to the companion's perturbing tidal field. The tidal deformability can be expressed through compactness $C = M/R$ and Love number k_2 . Here, M and R are the star mass and radius, respectively. The relation is

$$k_2 = \frac{3}{2} \Lambda \left(\frac{M}{R} \right)^5. \quad (21)$$

The method to calculate k_2 can be found in Refs. [38, 62, 63]. The calculated results show that with the increase of chiral chemical potentials the tidal deformability decreases.

D. Comparison of the influence of vector channel and axial-vector channel

The increase of weight factor α and chiral chemical potential μ_5 has opposite effect on the stiffness of EOS. With the increase of α , the EOS will become hard, whereas with the increase of μ_5 , EOS will become soft. Therefore, the increase of μ_5 will reduce the maximum mass in the mass-radius plot. A comparison of the mass-radius relation with different α and μ_5 is showed in Fig. 8 and the tidal deformabilities for a $1.4 M_\odot$ quark star are listed in Table I.

In addition, the increase of α will lead to the phase transition

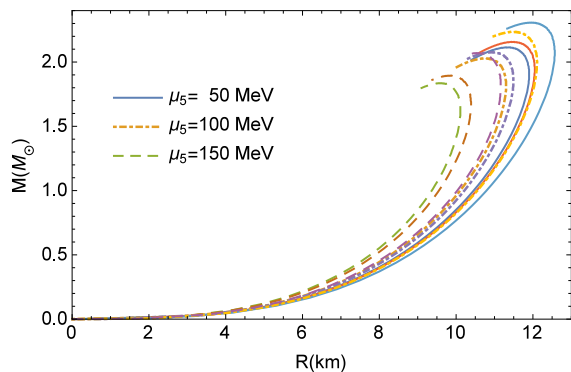


FIG. 8: Mass-radius relations for different α and μ_5 . When μ_5 is fixed, the maximum mass increases with α . Lines with the same μ_5 are corresponding to $\alpha = 0.5, 0.6,$ and 0.8 , respectively.

TABLE I: The tidal deformability of $1.4 M_\odot$ quark star for different α and μ_5 (MeV) .

$\alpha \backslash \mu_5$	50	100	150
0.5	606.198	450.802	226.158
0.6	648.325	497.448	271.404
0.8	790.556	654.638	421.616

from first-order to crossover, whereas μ_5 will lead to the transition from crossover to first-order. It seems that the effects of the two parameters may cancel each other out. When we think about them at the same time, we can not tell which factor (vector channel and chiral imbalance) plays the main role. However, the existence of μ_5 may affect the shape of mass-radius relationship. That is to say, without considering other external parameters, but constraining EOS by the maximum mass or tidal deformability from astronomical observation, the shape of mass-radius curves by including vector channel and axial-vector channel may be different from the one only considering vector channels. As can be seen from Fig. 9, our calculations confirm this. When the maximum masses are limited to about $2 M_\odot$, the radii corresponding to the maximum mass and the mass-radius curves are still different. The introducing of chiral chemical potential can make the tidal deformability have a right value. If we restrict the tidal deformability for a $1.4 M_\odot$ star to the range $70 < \Lambda(1.4 M_\odot) < 580$ [64, 65], the calculated tidal deformabilities with large α and small μ_5 is out of the range. That is to say, for quark stars when other parameters (such as magnetic field strength, rotation speed, temperature) are well understood, it is possible to observe the effectiveness of chiral chemical potential by analyzing the mass-radius relation and tidal deformability, so as to indirectly prove the violation of strong CP in compact stars.

IV. SUMMARY

The chiral imbalance indicates the nonequal density of left- and right- quarks that may occur in the QGP phase. In this

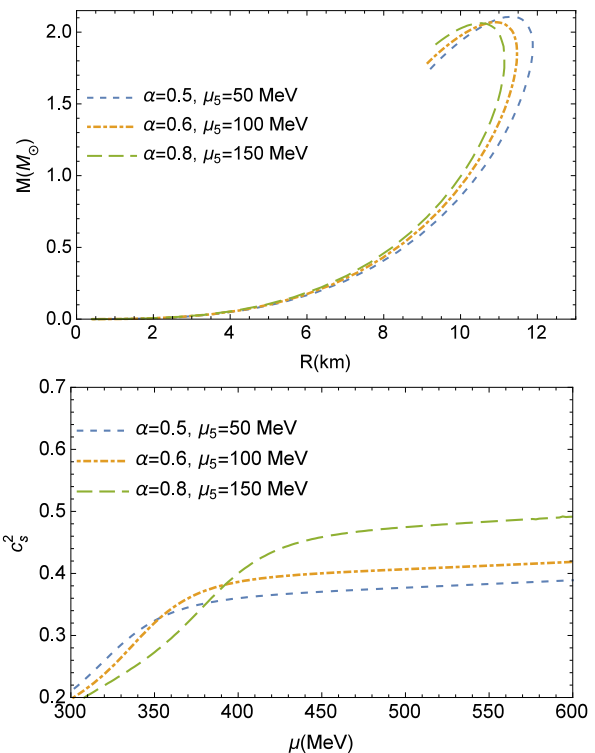


FIG. 9: Mass-radius relations and squared speed of sound. The mass-radius lines are setting to have almost equal maximum but the mass-radius relations and squared speed of sound c_s^2 are different which can be identified indirectly as a signal of CP violation inside the compact stars.

paper, we study the influence of chiral chemical potential μ_5 on the chiral phase transition and the EOS of quark matter. We use two-flavor NJL model with proper-time regularisation. And we know that there is no first-order phase transition at $\mu_5 = 0$ in this regularisation scheme. When μ_5 increases, the first-order phase transition appears. But the phase transition is not very strong. So it is difficult to find the position of CEP. On the other hand with fixed μ , the chiral phase transition responding to chiral chemical potential μ_5 is found to be a first-order phase transition, i.e., the CEP₅ exists.

We have calculated the pseudocritical temperature T_c and (pseudo-)critical chemical potentials μ_c as a function of μ_5 . It is found that these quantities increase rather than decrease with μ_5 . This is different to the result from three-momentum cutoff schemes. Besides, there are two maxima for the chiral susceptibility χ_μ at zero temperature. With the increase of μ_5 , the two maxima gradually approach to each other. In addition, we have also calculated the chiral susceptibility χ_μ at different temperatures. It is found that with the increase of temperature, the peaks gradually disappear and only the bumps remain. This further confirmed the existence of CEP when μ_5 is not zero. At last, we have calculated the EOS of quark matter and the mass-radius relation at different μ_5 . The calculations show that the EOS becomes soft with the increase of μ_5 . When parameters are set so that the maximum mass of quark stars is larger than $2M_\odot$, it is found that with

the increase of μ_5 , the maximum mass decreases gradually to masses far less than $2M_\odot$ and the maximum radius is less than 10 km .

We have also showed that when the mass-radius relations are constrained by maximum mass, the different radius that corresponding to the maximum mass and the variety of the mass-radius cures can be used to as a confirmation of the existence of chiral imbalance and indirectly prove the violation of strong CP in dense matter. However, this depends on the accurate measurement of the radius of compact star.

In conclusion, the chiral imbalance has significant influence on the chiral phase structure of quark matter. Since the chiral imbalance may possibly exist in the QGP phase, it is important

to consider it when confirm and locate the position of CEP in the experiments.

Acknowledgments

This work is supported in part by the National Natural Science Foundation of China (under Grants No. 11475085, No. 11535005, No. 11690030, No.11873030, and No. 11905104) and the National Major state Basic Research and Development of China (Grant No. 2016YFE0129300).

-
- [1] K. Rajagopal, F. Wilczek, "At the Frontier of Particle Physics / Handbook of QCD", Vol. 3 (World Scientific, 2001).
- [2] M. Buballa, Phys. Rep. **407**, 205 (2005).
- [3] K. Fukushima and T. Hatsuda, Rep. Prog. Phys. **74**, 014001 (2011).
- [4] X. F. Luo, and N. Xu, Nucl. Sci. Tech. **28**, 112 (2017).
- [5] Z. Fodor and S. D. Katz, J. High Energy Phys. **0203**, 014(2002).
- [6] R. V. Gavai and S. Gupta, Phys. Rev. D **71**, 114014 (2005).
- [7] G. 't Hooft, Phys. Rev. Lett. **37**, 8 (1976);
- [8] E. Witten, Nucl. Phys. B156, 269 (1979);
- [9] M. C. Chu, J. M. Grandy, S. Huang, and J. W. Negele, Phys. Rev. D **49**, 6039 (1994); C. Michael and P. S. Spencer, Phys. Rev. D **52**, 4691 (1995).
- [10] D. J. Gross, R. D. Pisarski, and L. G. Yaffe, Rev. Mod. Phys. **53**, 43 (1981).
- [11] T. Schafer and E. V. Shuryak, Rev. Mod. Phys. **70**, 323(1998)
- [12] P. Arnold and L. D. McLerran, Phys. Rev. D **36**, 581 (1987).
- [13] S. L. Adler, Phys. Rev. **177**, 2426 (1969).
- [14] N. H. Christ, Phys. Rev. D **21**, 1591 (1980).
- [15] A. V. Smilga, Phys. Rev. D **45**, 1378 (1992).
- [16] D. E. Kharzeev, Phys. Lett. B **633**, 260 (2006).
- [17] D. E. Kharzeev, L. D. McLerran, and H. J. Warringa, Nucl. Phys. A **803**, 227 (2008).
- [18] D. Kharzeev, R. D. Pisarski, and M. H. G. Tytgat, Phys. Rev. Lett. **81**, 512 (1998).
- [19] D. E. Kharzeev, Annals Phys. **325**, 205 (2010).
- [20] Kenji Fukushima, Dmitri E. Kharzeev, and Harmen J. Warringa PHYSICAL REVIEW D **78**, 074033 (2008)
- [21] M. Ruggieri, Phys. Rev. D **84**, 014011 (2011).
- [22] L. -K. Yang, X. Luo, and H. -S. Zong, Phys. Rev. D **100**, 094012 (2019).
- [23] Y. Lu, Z.-F. Cui, Z. Pan, C. -H. Chang, and H. -S. Zong, Phys. Rev. D **93**, 074037 (2016).
- [24] M. Asakawa and K. Yazaki, Nucl. Phys. A **504**, 668 (1989).
- [25] S. -X. Qin, L. Chang, H. Chen, Y. -X. Liu, and C. D. Roberts, Phys. Rev. Lett. **106**, 172301 (2011).
- [26] C. S. Fischer, Prog. Part. Nucl. Phys. **105**, 1 (2019)
- [27] Y. Hatta and M. A. Stephanov, Phys. Rev. Lett. **91**, 102003 (2003).
- [28] R. A. Lacey, N. N. Ajitanand, J. M. Alexander, P. Chung, W. G. Holzmann, M. Issah, A. Taranenko, P. Danielewicz, and H. Stcker, Phys. Rev. Lett. **98**, 092301 (2007).
- [29] L. Adamczyk *et al.* (STAR Collaboration), Phys. Rev. Lett. **112**, 032302 (2014).
- [30] B. Abelev *et al.* (ALICE Collaboration), Int. J. Mod. Phys. A **29**, 1430044 (2014).
- [31] E. R. Most, L. J. Papenfort, V. Dexheimer *et al.*, Phys.Rev.Lett. **122**, 061101 (2019).
- [32] M. G. Orsaria, G. Malfatti, M. Marianio *et al.*, J. Phys. G **46**, 073002 (2019).
- [33] M. Hanauske, L. Bovard, E. Most, J. Papenfort, J. Steinheimer, A. Motornenko, V. Vovchenko, V. Dexheimer, S. Schramm, and H. Stocker, Universe, **5**, 156 (2019).
- [34] A. Bauswein *et al.* AIP Conf. Proc. **212**, 020013(2019)
- [35] M. Ruggieri, Z. Y. Lu, and G.X. Peng, Phys. Rev. D **94**, 116003 (2016).
- [36] Q. Y. Wang, T. Zhao, and H. S. Zong, arXiv: 1908.01325.
- [37] T. Zhao, W. Zheng, F. Wang, C. M. Li, Y. Yan, Y. F. Huang, and H. S. Zong, Phys. Rev. D **100**, 043018 (2019).
- [38] Q. Wang, C. Shi, and H. S. Zong, Phys. Rev. D **100**, 123003 (2019).
- [39] S. P. Klevansky, Rev. Mod. Phys. **64**, 649 (1992).
- [40] R. Gatto and M. Ruggieri, Phys. Rev. D **85**, 054013 (2012).
- [41] F. Wang, Y. Cao, and H.-S. Zong, Chin. Phys. C **43**, 084102 (2019).
- [42] T. Kunihiro and R. Hatsuda, Prog. Theor. Phys. **74**, 765 (1985).
- [43] Z. -F. Cui, J. -L. Zhang, and H. -S. Zong, Sci. Rep. **7**, 45937 (2017).
- [44] P. Elmfors, D. Persson, and B. S. Skagerstam, Phys. Rev. Lett. **71**, 480 (1993).
- [45] D. Persson and V. Zeitlin, Phys. Rev. D **51**, 2026 (1995).
- [46] D. Ebert, K. G. Klimenko, M. A. Vdovichenko, and A. S. Vshivtsev, Phys. Rev. D **61**, 025005 (1999).
- [47] T. Inagaki, D. Kimura, and T. Murata, Prog. Theor. Phys. **111**, 371 (2004).
- [48] G. S. Bali, F. Bruckmann, G. Endrodi, Z. Fodor, S. D. Katz, and A. Schafer, Phys. Rev. D **86**, 071502 (2012).
- [49] Q. -W. Wang, Z. -F. Cui, and H. -S. Zong, Phys. Rev. D **94**, 096003 (2016).
- [50] D. Blaschke, H. Grigorian, and D. N. Voskresensky, Phys. Rev. C **88**, 065805 (2013).
- [51] D. E. Alvarez-Castillo and D. Blaschke, Phys. Part. Nucl. **46**, 846 (2015).
- [52] U. H. Gerlach, Phys. Rev., **172**, 1325 (1968).
- [53] M. A. R. Kaltenborn, Niels-Uwe F. Bastian, D. B. Blaschke, Phys. Rev. D **96**, 056024 (2017).
- [54] S. Benic and D. Blaschke, D. E. Alvarez-Castill, T. Fischer, and S. Typel, Astron. Astrophys., **577**, A40 (2015).
- [55] H. S. Zong, W. M. Sun, Phys. Rev. D **78**, 054001 (2008).
- [56] H. S. Zong, W. M. Sun, Int. J. Mod. Phys. A **23**, 3591 (2008).

- [57] P. Demorest, T. Pennucci, S. M. Ransom, M. S. E. Roberts, and J. W. T. Hessels, *Nature* **467**, 1081 (2010).
- [58] J. Antoniadis *et al.*, *Science* **340**, 1233232 (2013).
- [59] E. Fonseca, T. T. Pennucci, J. A. Ellis, I. H. Stairs, D. J. Nice, S. M. Ransom, P. B. Demorest, *et al.*, *Astrophys. J.* **832**, 167 (2016).
- [60] H. T. Cromartie *et al.*, *Nat. Astron.*, 10.1038/s41550-019-0880-2 (2019).
- [61] N. K. Glendenning, "Compact stars", Springer, New York, (1997).
- [62] T. Damour and A. Nagar, *Phys. Rev. D* **80**, 084035 (2009).
- [63] C. M. Li, S. Y. Zuo, Y. Yan *et al.*, *Phys. Rev. D* **101**, 063023 (2020).
- [64] B. P. Abbott *et al.*, *Phys. Rev. Lett.* **119**, 161101 (2017); *Phys. Rev. Lett.* **121**, 161101 (2018).
- [65] E. Annala, T. Gorda, A. Kurkela *et al.*, *Nat. Phys.*, 10.1038/s41567-020-0914-9 (2020)